

<https://doi.org/10.1038/s43247-024-01670-7>

# Antarctic meltwater reduces the Atlantic meridional overturning circulation through oceanic freshwater transport and atmospheric teleconnections

Check for updates

Soon-Il An<sup>1,2</sup>✉, Jun-Young Moon<sup>1,2</sup>, Henk A. Dijkstra<sup>3</sup>, Young-Min Yang<sup>4</sup> & Hajoon Song<sup>1,2</sup>

The Atlantic meridional overturning circulation is an important component of the climate system because of its role in the heat transport. Its strength is sensitive to the surface density but mechanisms of the effect of Southern Ocean freshwater anomalies are relatively unknown. Here, we investigate the impact of Antarctic ice sheet meltwater on the Atlantic meridional overturning circulation using an earth system model of intermediate complexity. The meltwater over the Pacific sector of the Southern Ocean is transported to the east and, after passing the Drake Passage, travels northward reaching the North Atlantic. Furthermore, Southern Ocean cooling induces a northward shift of the Intertropical Convergence Zone, leading to more precipitation in the tropical Atlantic. Consequently, the reduced salinity weakens the Atlantic meridional overturning circulation. Additional experiments, in which the duration period of freshwater hosing was varied while keeping its total amount constant, indicate that the amplitude and the duration of the meltwater play crucial roles in determining the degree of reduction in Atlantic meridional overturning circulation.

The Earth's continents act as dividers within the global ocean, creating separate ocean basins; however, these ocean basins are interacting through the global ocean circulation and atmospheric teleconnections. A hemispheric oceanic interaction operates through the Atlantic meridional overturning circulation (AMOC)<sup>1,2</sup>. Both the intensity of the AMOC and the formation of Antarctic Bottom Water (AABW), constituting the global abyssal circulation, are currently undergoing reduction because of freshening and warming associated with global warming<sup>3-6</sup>.

Two continental ice sheets, Greenland (GrIS) and West Antarctic (WAIS) have been suggested to undergo tipping by a future 1.5 °C global warming<sup>7</sup>. Resultant massive meltwater is anticipated to flow into the North Atlantic and the Southern Ocean (SO). As a result, the AMOC and the AABW are expected to slow down due to ocean surface freshening resulting from melting of the continental ice sheets. However, the transition timescale of WAIS (2000 years) is about five times faster than that of GrIS (10,000 years)<sup>7</sup>, prompting a natural question of whether the melting of WAIS induces change in the AMOC before substantial melting occurs in GrIS.

Previous studies<sup>8-13</sup> have indicated that the discharge of Antarctic meltwater induces a regional cooling of the surface ocean. For example, SO surface cooling of ~1 °C was found when a freshwater flux of about 0.5 Sv was applied over the SO for a duration of 350 years in the UK Met Office's Hadley Centre Coupled Model version 3<sup>1</sup>. This cooling is driven by a combination of factors, including rapid mixing facilitated by the Antarctic Circumpolar Current (AAC), northward Ekman transport induced by the westerlies, and leads to increased sea ice production. The meltwater over the SO is also causing freshening of the Antarctic Intermediate Water as well as a deepening of the SO pycnocline, which, in turn, strengthens the AMOC by enhancing the subsurface-meridional density gradient<sup>2</sup>. On the other hand, the negative surface salinity anomalies originating from the SO can be transported to the North Atlantic, hindering the formation of North Atlantic Deep Water (NADW)<sup>11</sup>. The dominant process among these two opposing effects on the AMOC associated with the SO surface freshening is dictated by the quantity of added freshwater and its duration<sup>10,12</sup>. The optimal threshold for the amount of freshwater may not be easily determined but Swingedouw et al.<sup>13</sup> suggested that freshwater input lower than

<sup>1</sup>Irreversible Climate Change Research Center, Yonsei University, Seoul, Republic of Korea. <sup>2</sup>Department of Atmospheric Sciences, Yonsei University, Seoul, Republic of Korea. <sup>3</sup>Department of Physics, Utrecht University, Utrecht, The Netherlands. <sup>4</sup>Joint International Research Laboratory of Climate and Environment Change and Key Laboratory for Prevention of Meteorological Disaster, Ministry of Education, Nanjing University of Information Science and Technology, Nanjing, China. ✉e-mail: [sian@yonsei.ac.kr](mailto:sian@yonsei.ac.kr)

0.1–0.2 Sv in the SO enhances the AMOC strength through deep-water adjustment, whereas an input exceeding 0.1–0.2 Sv suppresses the AMOC by spreading salinity anomalies<sup>11</sup>. Additionally, these two processes operate on different timescales, with the deep-water adjustment taking place over a few years, faster than the salinity spreading process, which spans a few decades. Therefore, the impact of Antarctic ice sheet (AIS) melting on the AMOC is thought to depend on both the amount and duration of the melting. Nevertheless, the influence of freshwater over the ACC region on the AMOC remains unclear so far.

The AIS, reaching a thickness of nearly 4.9 km and containing about 30 million cubic kilometers of ice, holds the potential to cause a sea-level rise of ~60 m if it were to completely melt. Under the Intergovernmental Panel on Climate Change (IPCC) scenario SSP5.8.5, the disintegration of major Antarctic ice shelves by the end of the century, combined with increased ice discharge, could lead to a catastrophic sea-level rise of 9–10 m by the year 2300<sup>14</sup>. This corresponds to an approximate meltwater input of 1.0 Sv into the ocean over a period of 100 years, which accounts for about 10% of the current total Antarctic ice sheet. This input of meltwater into the Southern Ocean is expected to strongly contribute to changes of the AMOC.

The primary objective of this study is to address the question of how the AIS melting influences the AMOC and, consequently, the global climate. This question is somewhat related to cascading tipping, i.e., whether the tipping of the AIS can trigger a tipping in the AMOC. A key process on this tipping cascade involves the largest global-scale interaction, sometimes called as the bipolar seesaw, especially between the Arctic including the North Atlantic and the Antarctic<sup>11,12,15,16</sup>. Moreover, due to the complexity of the SO climate system, the response of the AMOC to AIS melting may vary depending on the meltwater input location in the SO. Therefore, we examine the influence of AIS melting on the AMOC using a coupled atmosphere-ocean model of intermediate complexity (LOVECLIM), of which the overall performance of AMOC behavior under freshwater forcing has been well studied (see section “Methods”). We conducted hosing experiments, where a total freshwater pulse of 1.0 Sv is introduced on five distinct sectors of SO for 100 years evenly over each designated sector and followed by shutting off the freshwater pulse (standard hosing experiment). Although the geographical areas of each sector are different, the total amounts of the imposed freshwater are the same. Here, all results are an average of 10 ensemble members, and a simulation under the pre-industrial conditions without hosing is considered as the control experiment (see Table 1).

Here, we demonstrated that freshwater spreading from SO to the North Atlantic, combined with enhanced precipitation in the northern tropical Atlantic due to SO surface cooling via atmospheric teleconnections, reduces surface salinity in the North Atlantic. This subsequently leads to a reduction in the AMOC. The extent of AMOC reduction depends on the locations of hosing, with hosing over the Pacific sectors of SO having a more pronounced effect. Finally, we found that both the hosing rate and duration play crucial roles in determining the rate of AMOC reduction.

## Results

### AMOC response to Antarctic meltwater pulse

The five distinct sectors in SO chosen for hosing are Wilkes Land, Ross Sea, Amundsen Sea, Bellingshausen Sea, and Weddell Sea (Fig. 1a). The Ross, Amundsen, and Bellingshausen Seas are in Pacific sector; the Weddell Sea is in the Atlantic sector; and Wilkes Land is in between the Indian and Pacific Oceans. Regardless of hosing location, the freshening in the SO by adding 1 Sv of freshwater for 100 years (see Table 1) leads to a weakening of the AMOC (Fig. 1b). In our hosing experiments, we applied an ocean volume compensation to conserve the global volume mean salinity. However, the standard hosing experiment without the volume compensation produced a negligible difference in AMOC response compared to that with the volume compensation (Fig. S1). Following the input of freshwater, the AMOC experiences a slight intensification for the first 30 years, followed by a pronounced decrease until ~200 years, reaching its minimum. Subsequently, a recovery phase occurs, taking about 100 years to get a full recovery from its minimum state. The AMOC response to the Antarctic meltwater pulse depends on the amount of freshwater per unit time introduced<sup>12</sup>. In case of the freshwater forcing of 0.1 Sv for 100 years (Fig. 1c), there is a modest initial increase in the AMOC during the period of freshwater addition. However, this is followed by a slight declining trend that persists for over 150 years before the AMOC eventually recovers. For freshwater forcing of 0.5 Sv, the response of AMOC mirrors that for a 1.0 Sv forcing, but with a less pronounced amplitude (Fig. 1d).

An interesting aspect of this experiment is the sensitivity of the AMOC response to the specific region where freshwater is introduced. The results demonstrate that freshwater forcing in the Pacific sector, specifically in the Ross, Amundsen, and Bellingshausen Seas, leads to more than a 20% decrease in the AMOC intensity, which is more efficient than that from the input of freshwater in the other two regions, namely the Weddell Sea and Wilkes Land (as shown in Fig. 1b, d). Although the addition of freshwater to regions in the Pacific sector and the other regions display a similar pattern in AMOC behavior, they cause distinct AMOC responses. The regions in the Pacific sector, which show a more pronounced effect on the AMOC, are identified as the high-impact group (HIG), while the other two regions, which have a lesser impact on AMOC, are labeled as the low-impact group (LIG).

The weakening of the AMOC is more pronounced after the cessation of hosing than during the water hosing period (1–100 years) itself. Here, we present the global meridional overturning circulation (GMOC) and the AMOC averaged over the years 101–200, derived from the composites of both HIG and LIG (Fig. 2). In both HIG and LIG, a slowdown of the GMOC is observed. The weakening of both the upper ocean cell (centered near 50° N at a depth of 1000 m) and the lower deep ocean cell (centered at 40° S and at a depth of 4000 m) results from the SO hosing. This pattern of weakening aligns with the observed changes in the GMOC over recent decades, which includes a decrease in the southward returning flow of the lower NADW and a reduction in the AABW associated with SO freshening and warming<sup>17</sup>. The changes in the upper cell of the GMOC can be fully explained by changes in the AMOC (Fig. 2c, d). The weakening of AABW formation has

**Table 1 | Experimental design**

	Hosing rate (Sv)	Hosing duration (year)	Hosing location
Control experiment	N/A	N/A	N/A
Standard hosing experiment	1.0	100	Southern Ocean
Different hosing rate experiments	0.1	100	Southern Ocean
	0.5	100	Southern Ocean
Different hosing rate/duration experiment	0.5	200	Southern Ocean
	2.0	50	Southern Ocean
	4.0	25	Southern Ocean
Fixed precipitation experiment	1.0	100	Southern Ocean (precipitation fixed over Atlantic Ocean of 0–30° N)

Summary of experimental designs.

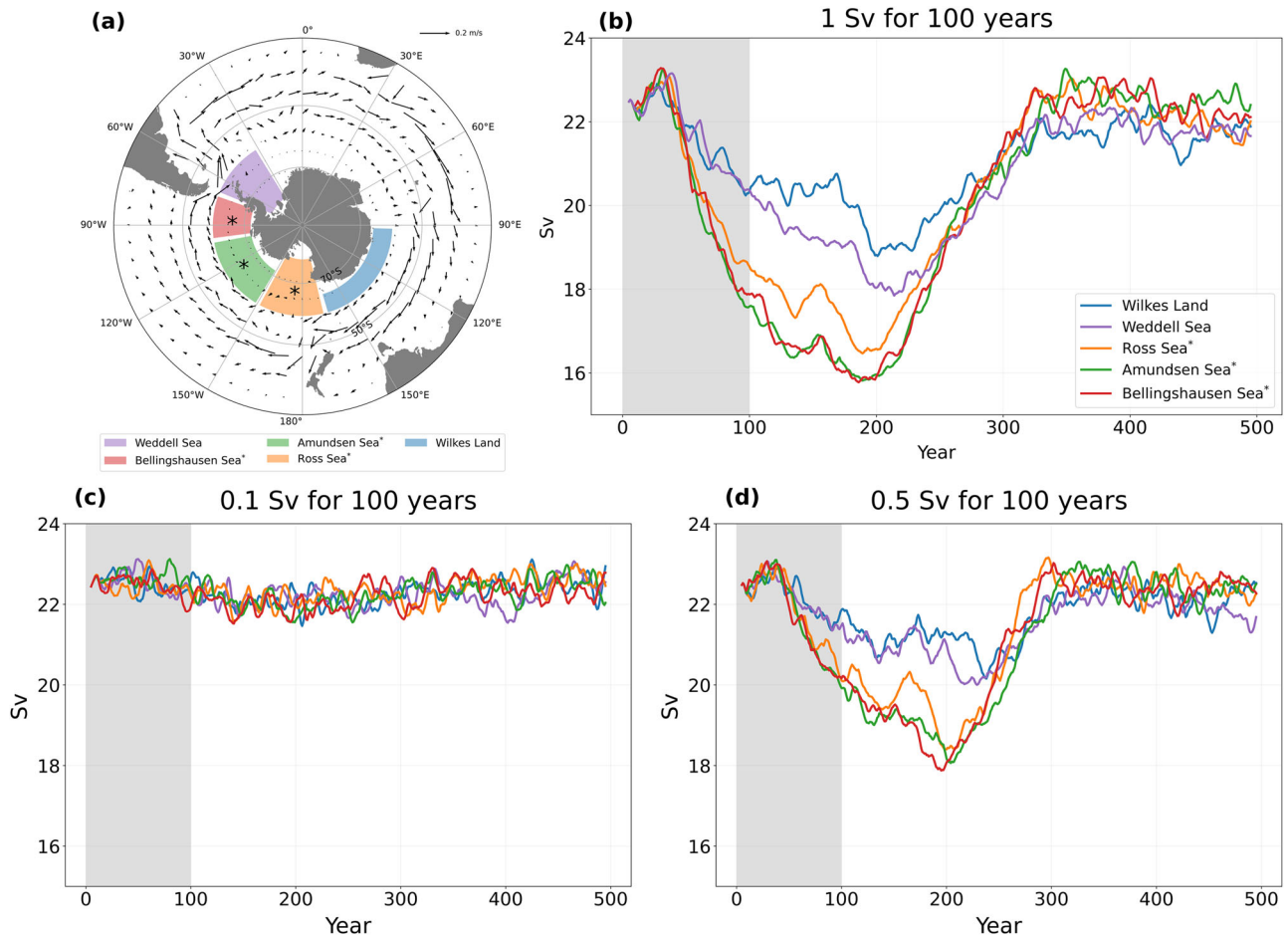


**Fig. 1 | AMOC response.** **a** Freshwater forcing regions over the Southern Ocean marked by different colored boxes, and climatological mean upper ocean currents from the control experiment. Names of each box are found at the bottom of the panel. Vector scales for the current is marked in the upper right corner. **b** Response of 10-year moving averaged AMOC index to the freshwater forcing of 1.0 Sv for 100 years adopted over the Southern Ocean. The AMOC index indicates the maximum

of annual mean meridional overturning stream function (Sv) north of 20° N, below 500 m in the Atlantic Ocean. The area of the imposed freshwater is indicated as the different colored line as indicated in the lower right corner. The hosing periods are indicated by a light gray shading. The star mark (\*) in each panel indicates member of high-impact group, otherwise low-impact group. **c, d** As in (a) but for 0.1 Sv for 100 years and 0.5 Sv for 100 years, respectively.

been suggested to enhance AMOC strength by intensifying the subsurface-meridional density gradient<sup>1,2,12</sup>. However, as depicted in Fig. 2c, d, the changes deeper than 3000 m associated with the AABW in the Atlantic Ocean are weak. Therefore, these minor alterations in the deep ocean circulation in the Atlantic sector may not be strong enough to induce a strengthening of the AMOC. Additionally, the changes in the meridional density gradient in the upper ocean averaged from the surface to 1000 m depth, as a result of SO hosing, are weak compared to the control experiment for the early hosing periods (Fig. S2a, b), which is indicative of a weakening of the AMOC. This is particularly found in the experiments involving HIG.

**AMOC slowdown due to oceanic transport**

The influx of low salinity water from the SO into the North Atlantic could lead to a slowdown of the AMOC by enhancing surface buoyancy forcing. As shown in Fig. 3a, the sea surface salinity (SSS) in the northern tropical Atlantic (0°–30° N) decreases during the hosing period (year from 1 to 100), reaching its lowest point around model year 110–120, before returning to its original state over the following 100 years. The reduction in SSS is much more pronounced in HIG compared to LIG. The SSS changes in the high-latitude North Atlantic (45°–65° N) exhibit a rather slow decline, with the lowest values appearing around model year 200 (Fig. 3b). Therefore, their temporal behaviors resemble that of the AMOC change (Fig. 1b).

The substantial decrease in salinity by the meridional salinity convergence in the mixed layer (see section “Methods”) over the high-latitude

North Atlantic (45°–65° N) is found up to 150 years (Fig. 3d). This reduction is due to decreases in both salinity and ocean currents (Fig. 1b, d). Prior to the high-latitude salinity reduction, the negative salinity flux convergence in the tropical Atlantic (0°–30° N) was maximized (Fig. 3c), indicating a sequential northward transport of low salinity water. In addition to the salinity transport, the surface salinity flux also contributes the reduction in SSS over North Atlantic (Fig. 3e, f). It’s noteworthy that in the tropical Atlantic, the negative surface salinity flux and the negative salinity flux convergence happen concurrently. However, in the high-latitude region, a negative surface salinity flux occurs after the return of the negative salinity flux convergence to normal conditions. Thus, a shorter timescale and strong response to the hosing is observed in the tropical Atlantic, while the longer timescale response is observed in the high-latitude region.

A series of snapshots of the 10-year mean SSS changes with an interval of about 50-year shows the transport of low salinity waters (Fig. 4). Here, the “change” indicates the deviation from the control experiment. In the early period of the HIG simulations (Ross Sea, Amundsen Sea, and Bellingshausen Sea), the low salinity water is mainly confined within the Pacific sector of the high-latitude SO. Once this water traverses the Drake Passage, it rapidly disperses throughout the entire Atlantic Ocean. Specifically, the Falkland current (Fig. 1a) carries the low salinity water towards the equator along the South American east coast (see years 11–20 of Fig. 4), and some of this water spreads into the South Atlantic Ocean due to the returning flow of the eastward South Atlantic Current (see years 51–60 of Fig. 4). At the same

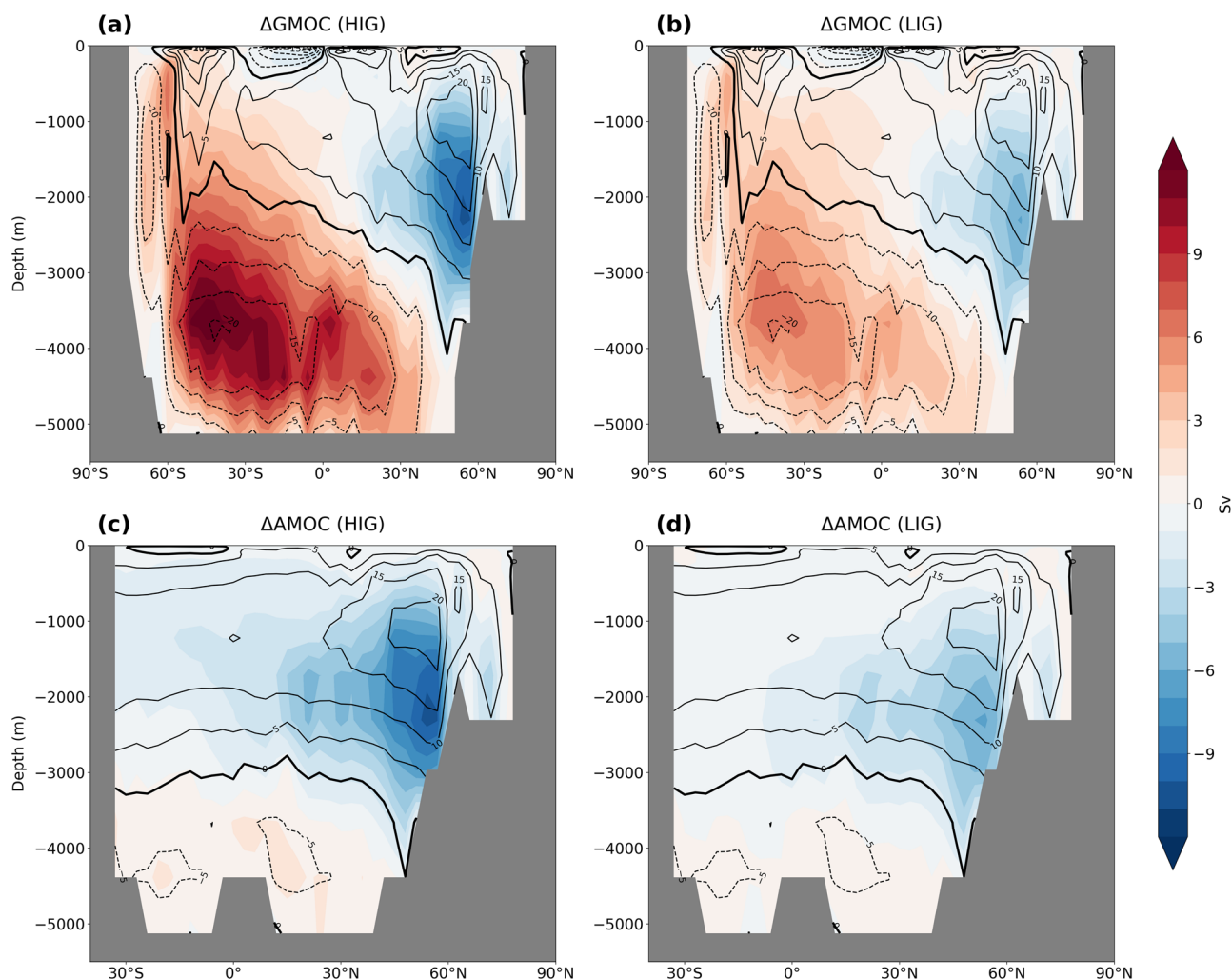


**Fig. 2 | Meridional overturning circulations.** **a** Latitude–depth section of the difference (color-shading) in the global meridional overturning circulation stream function (unit: Sv) between the results from the high-impact group (average over years 101–200) and control experiment (average over whole period). **b** As in (a)

except the result from the low-impact group. **c, d** Same as in (a) and (b), respectively, but only the stream function of the Atlantic Ocean north of 30° S is shown. Contours in all figures indicate the corresponding mean values from the control experiment, in which contour interval is 5 Sv.

time, the northern tropical Atlantic becomes fresher because of enhanced precipitation (Figs. 3e and 5c, d). The salinity in the northern tropical Atlantic is reduced further due to advected low salinity water along the coast (years 91–100 of Fig. 4). The Gulf Stream and then the North Atlantic Current carry the low salinity water into the NADW formation region (111–120 years of Fig. 4). Since the advective timescale to pass between hemispheres is several decades, the salinity levels in the North Atlantic Ocean experience a further decrease and reach their minimum values in several decades after the cessation of the freshwater input. Then they slowly begin to return to their previous levels (Fig. 3b). It should be emphasized that the freshening of the Atlantic Ocean does not occur evenly in space. Specifically, the reduction in salinity is more pronounced in the western region of the South Atlantic Ocean and the northern part of the tropical Atlantic because of mean ocean circulations.

The low salinity water near Wilkes Land (LIG), situated between the Pacific and Indian Oceans, does not travel through the Drake Passage but instead spread across the South Pacific Ocean (top row of Fig. 4). Wilkes Land is located farther west than other hosing areas and thus, it is likely connected to the lower branch of Pacific subtropical gyre, which carries the low salinity water into the South Pacific basin (years 11–20 and 51–60 of Fig. 4). As a result, substantial freshening is observed in the southeastern Pacific, while the Atlantic Ocean exhibits small changes in salinity (Figs. 3a, b and 4). Likewise, the low salinity water originating from the

Weddell Sea moves zonally and reaches the Pacific sector of the SO, with only a small fraction moving into the Atlantic Ocean (second row of Fig. 4). This is because the freshwater in this region hardly traverses to the lower latitude ocean because of the strong ACC. Overall, the introduction of freshwater in both Wilkes Land and the Weddell Sea results in only minor salinity changes in the Atlantic Ocean, which in turn leads to a weak impact on the AMOC. In essence, the transit of low-salinity water through the narrow Drake Passage seems to be a critical factor for its movement across the Atlantic Ocean because the water passing through the passage meets the northward Falkland current.

#### North Atlantic freshening via atmospheric teleconnection

In addition to oceanic transport, there is also a potential impact of atmospheric teleconnections on the salinity changes in the Atlantic. Consistently with previous studies<sup>1,8–13</sup>, our simulations indicate that SO freshening leads to surface cooling due to diminished vertical heat transport from below, a consequence of enhanced oceanic stratification (Fig. S2a, b). During the freshwater hosing period (1–100 year), our simulations exhibit a SST cooling of ~2.5 °C in HIG and about 1.5 °C cooling in LIG, as compared to the control experiment, across the high-latitude SO belt (as shown in Fig. 5a and b, respectively). Meanwhile, a slight warming is observed in the Northern Hemisphere. Furthermore, the surface air temperature changes almost mirror that in SST but with a broader spread of the signal

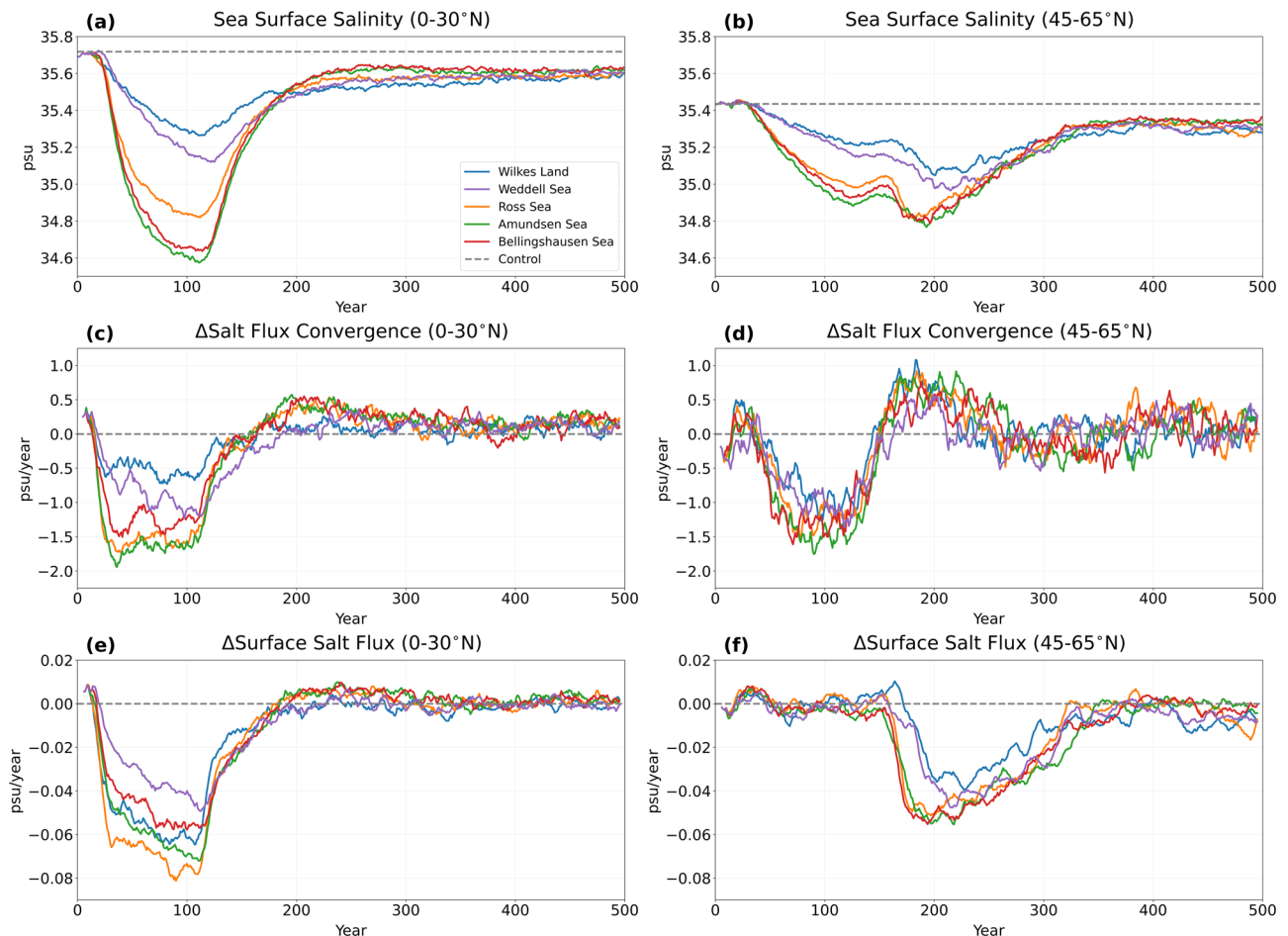


**Fig. 3 | Salinity change over Atlantic Ocean.** Time series of **a** sea surface salinity, **c** changes in horizontal salinity flux convergence in a mixed layer, and **e** changes in surface salinity flux averaged over 0°–30° N of North Atlantic Ocean (“Methods” section). Negative flux means loss of salinity. **b, d, f** As in (a), (c), (e), respectively, but

for the latitudes 45°–65° N of the North Atlantic Ocean. Units for salinity are practical salinity unit (psu); and salinity flux convergence and salt transport are psu year<sup>-1</sup>. All results are obtained from the standard hosing experiment.

(Fig. S3a, b). This hemispheric thermal contrast is likely to drive the northward migration of the Intertropical Convergence Zone (ITCZ), resulting in increased wetness in the northern tropics and dryness in the southern tropics (Fig. 5c, d). Note that the HIG exhibits stronger SO cooling, more precipitation in northern tropical oceans, and stronger westerly anomalies over the SO (Fig. S3c, d), compared to LIG. The enhanced westerlies over the SO induce increased northward Ekman transport. If this transport is balanced by a deep geostrophic current, such as NADW export<sup>18</sup>, these intensified westerly anomalies may potentially increase AMOC intensity. However, our results suggest that even if this wind effect is present, the impact of low salinity water spreading has a stronger influence, ultimately overwhelming the wind-driven circulation effect.

The hemispheric contrast in surface pressure, characterized by higher pressure in the Southern Hemisphere and lower pressure in the Northern Hemisphere, further supports the northward shift of the ITCZ (Fig. 5c, d). Consequently, the increased precipitation in the northern tropics leads to reduced salinity in that region (Figs. 3a and 4). The surface salinity flux over the 0–30° N latitudinal band in the Atlantic Ocean also shows a decrease in surface salinity (Fig. 3e). This decrease in surface salinity flux is primarily attributed to an increase in precipitation, while changes in evaporation are negligible (Fig. S4). Furthermore, the evolutions of surface salinity flux over the 0–30° N latitudinal band in the Atlantic Ocean (Fig. 3e) closely follows the changes in precipitation (Fig. S5). Overall, the decrease in salinity within the northern tropical Atlantic results in decreased meridional salt transport over the high-latitude Atlantic (Fig. 3d), which in turn contributes to the weakening of the AMOC.

The relationship between SO cooling over the Pacific sector and surface salinity flux in the northern tropical Atlantic is approximately linear with a scaled regression coefficient of  $6.57 \times 10^{-3} \text{ psu yr}^{-1} \text{ } ^\circ\text{C}^{-1}$  (the regression coefficient multiplied by 35 psu reference salinity and divided by 100 m mixed-layer depth). It refers approximately that 1 °C SO cooling leads to the 0.66 psu reduction per 100 years (Fig. S6). Specifically, the change in salinity flux in the northern tropical Atlantic resulting from freshwater hosing over Wilkes Land (LIG), is more substantial than that from hosing over the Bellingshausen Sea (HIG) (Figs. 3e and S6). This distinction is attributed to a more pronounced cooling effect in the SO of the Pacific sector due to hosing over Wilkes Land compared to that from the Bellingshausen Sea. Despite this, the AMOC shows a stronger response to hosing over the Bellingshausen Sea than to Wilkes Land hosing (Fig. 1b). This difference in AMOC response can be explained by the stronger salinity meridional advection (i.e., salinity flux convergence) associated with Bellingshausen Sea hosing compared to that from the Wilkes Land hosing (Fig. 3d).

The atmospheric teleconnection effect driven by SO cooling is further examined by performing a sensitivity simulation, in which the precipitations in the latitude band 0°–30° N of the Atlantic Ocean are fixed as the climatological mean from the control experiment. Apart from that, the hosing is applied in the same manner as in the standard hosing experiment. In this way, the climatological precipitation in the northern tropical Atlantic is maintained and not affected by the SO hosing, with the rest of the model’s coupled climate system free to evolve.

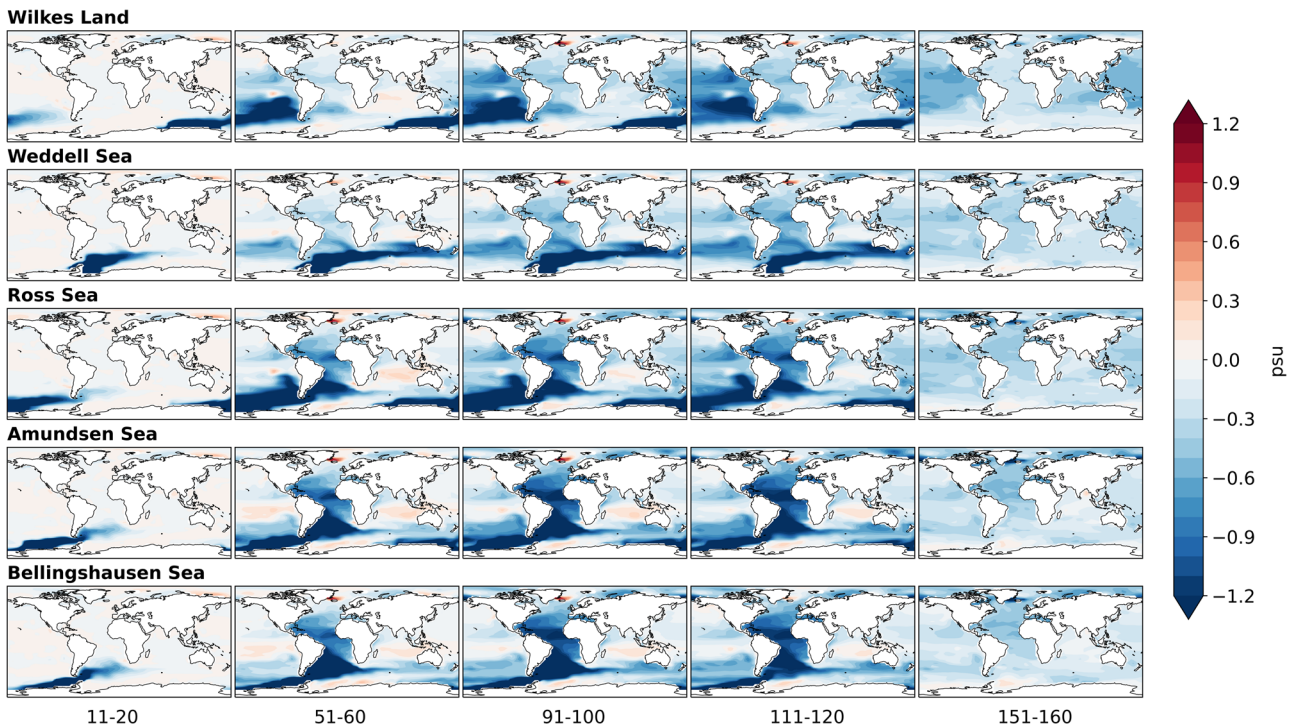


**Fig. 4 | Snapshot of global salinity.** Distributions of 10-year averaged surface salinity difference between the standard hosing experiments over Wilkes Land, Wendell Sea, Ross Sea, Amundsen Sea, and Bellingshausen Sea from top row to

bottom row, respectively, and the control experiment. Temporal averaging periods include model years 11–20, 51–60, 91–100, 111–120, and 151–160, from left to right. Units are psu.

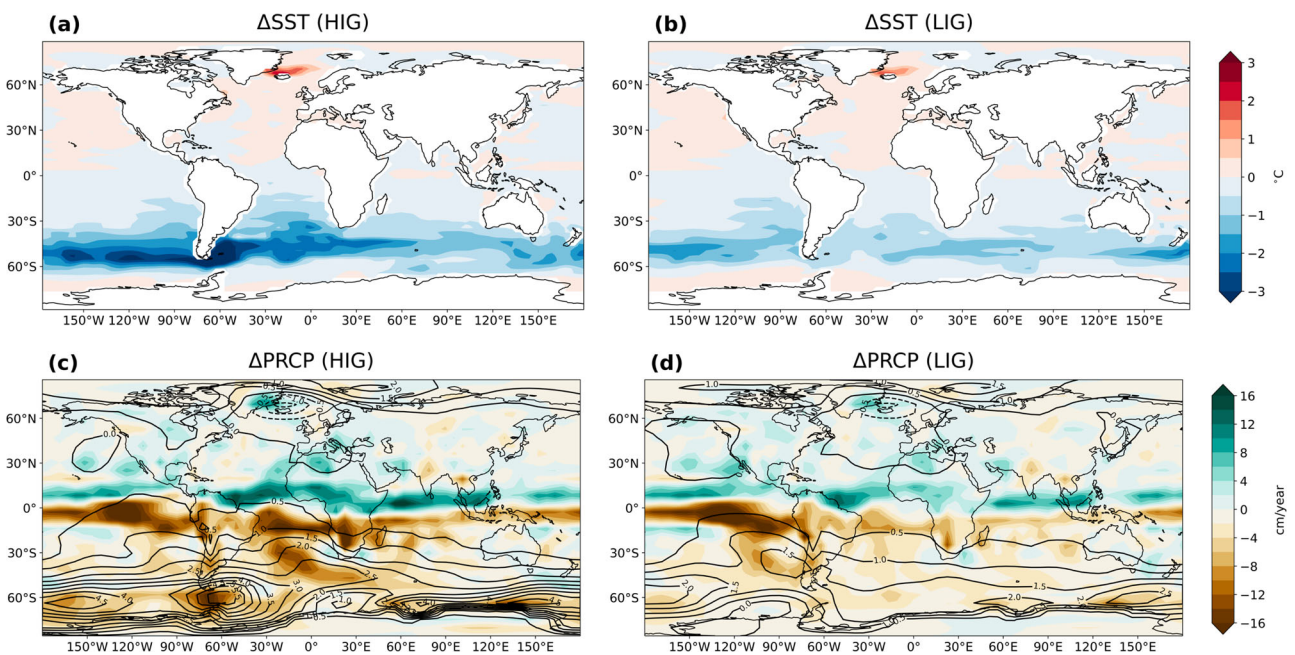


**Fig. 5 | SST and precipitation distributions.** Changes in the first 100-year average of sea surface temperature (unit: °C) for **a** HIG and **b** LIG. Here, the change indicates a deviation from the corresponding mean of the control experiment. **c, d** As in **(a)**

and **(b)**, respectively, expect for the changes in precipitation (shading, unit:  $\text{cm year}^{-1}$ ) and surface pressure (contours, unit:  $\text{hPa}$ ).

Therefore, we can isolate the effect of the advective freshwater transport from the atmospheric teleconnection effect. The results reveal an about 1–2 Sv increase of the mean AMOC over the period (years 175–225) when compared to the original hosing experiment without the precipitation nudging (Fig. S7). This indicates that 15–50% of the AMOC

reduction is likely due to the atmospheric teleconnection, especially through the freshening of the northern tropical Atlantic. Interestingly, the AMOC reductions caused by atmospheric teleconnection are dominant in LIG, accounting for about 35–50% of their total reduction, while those in HIG are about 15–20% of their total reduction.

### Sensitivity of AMOC response to the hosing timescale

To investigate the effects of the duration of hosing on AMOC, we conducted sensitivity experiments, in which the duration of freshwater hosing is varied, while maintaining its total amount (1.0 Sv  $\times$  100 years) constant: 0.5 Sv for 200 years, 2.0 Sv for 50 years, and 4.0 Sv for 25 years (Fig. 6). We found that the slower hosing (0.5 Sv for 200 years) strongly reduces AMOC response (Fig. 6a). This could be because slower freshening allows more time for the re-salinization process, aided by the ACC<sup>1</sup>, thereby reducing the impact of the freshwater spread into the Atlantic. We also found that in case of the faster hosing of 2.0 Sv for 50 years, the reduction in the AMOC becomes more pronounced, but the AMOC change by a further faster hosing of 4.0 Sv for 25 years is slightly weaker (Fig. 6c, d). This could be because the fast hosing (e.g., 4.0 Sv for 25 years) does not provide enough time for the AMOC to adjust. In other words, the response timescale of the AMOC is longer than the timescale of the forcing. Consequently, our findings suggest that a combination of suitable amount and duration of freshwater hosing over SO can lead to a maximal reduction in the AMOC.

### Discussions

Under a substantial freshening of the SO associated with the melting of the Antarctic ice sheet, there is a notable reduction in the intensity of the AMOC. Intriguingly, the most pronounced weakening in the AMOC is found with a delay of about 100 years. This weakening is primarily attributed to a decrease in salinity over the North Atlantic, which occurs through two mechanisms. First, the low salinity water introduced into the SO is transported through the Drake Passage and subsequently spreads northwards, reaching the North Atlantic and reducing its salinity. Secondly, the low salinity water in the SO leads to cooling in the region, thereby intensifying the hemispheric thermal contrast. This enhanced thermal contrast causes a northward shift of the ITCZ. As a result, there is an increase in precipitation over the northern tropical Atlantic, which further contributes to the reduction of northward salinity transport, impacting the strength of the

AMOC. Our research indicates that the response of the AMOC to SO hosing is highly sensitive to the location of freshwater input. Specifically, the Ross, Amundsen, and Bellingshausen Seas, located in the Pacific sector of the SO, are identified as areas where freshwater hosing most effectively leads to a reduction in the AMOC strength. In contrast, hosing over the Weddell Sea and Wilkes Land results in a relatively small reduction in AMOC strength.

In our study, northern hemispheric meltwater effects were not taken into account. For example, Meltwater Pulse 1a (MWP1a), the largest rapid global-mean sea-level rise event occurred around 14.6 thousand years ago<sup>19</sup>, resulted from a massive land-ice melting over North America, northeast Europe, and possibly Antarctica<sup>20</sup>. It has been argued that such massive northern hemisphere land-ice melting would overwhelm the effect of Antarctic ice sheet melting on AMOC<sup>1</sup>. Including additionally northern hemisphere ice sheet melting would have an impact on the AMOC, leading to a more complex response than that caused by freshwater forcing from a single hemisphere. However, in the present-day climate, only the Greenland Ice Sheet remains in the Northern Hemisphere, and thus the future potential meltwater pulses are quite different from the past. Therefore, a substantial melting of the Antarctic ice sheet alone can perturb the strength of AMOC as seen in this study. Furthermore, if the AMOC is markedly weakened without the melting of the Greenland Ice Sheet, this reduction in the AMOC could induce cooling in the North Atlantic and its adjacent areas. This cooling, in turn, may potentially slow down the melting of the Greenland Ice Sheet<sup>21</sup>. Nevertheless, the stabilizing effect of a weakened AMOC on the GrIS must compete with the destabilizing influence of global warming, as long as CO<sub>2</sub> concentrations continue to rise. However, it remains unclear which of these effects will ultimately be dominant.

A previous study<sup>16</sup>, using a simple model that conceptualizes the dynamics of the AMOC, GrIS, and WAIS, demonstrated that the tipping of the GrIS could induce AMOC tipping under a subcritical level of global warming that would typically trigger AMOC tipping. However, the abrupt collapse of the WAIS hindered AMOC tipping by reducing the meridional

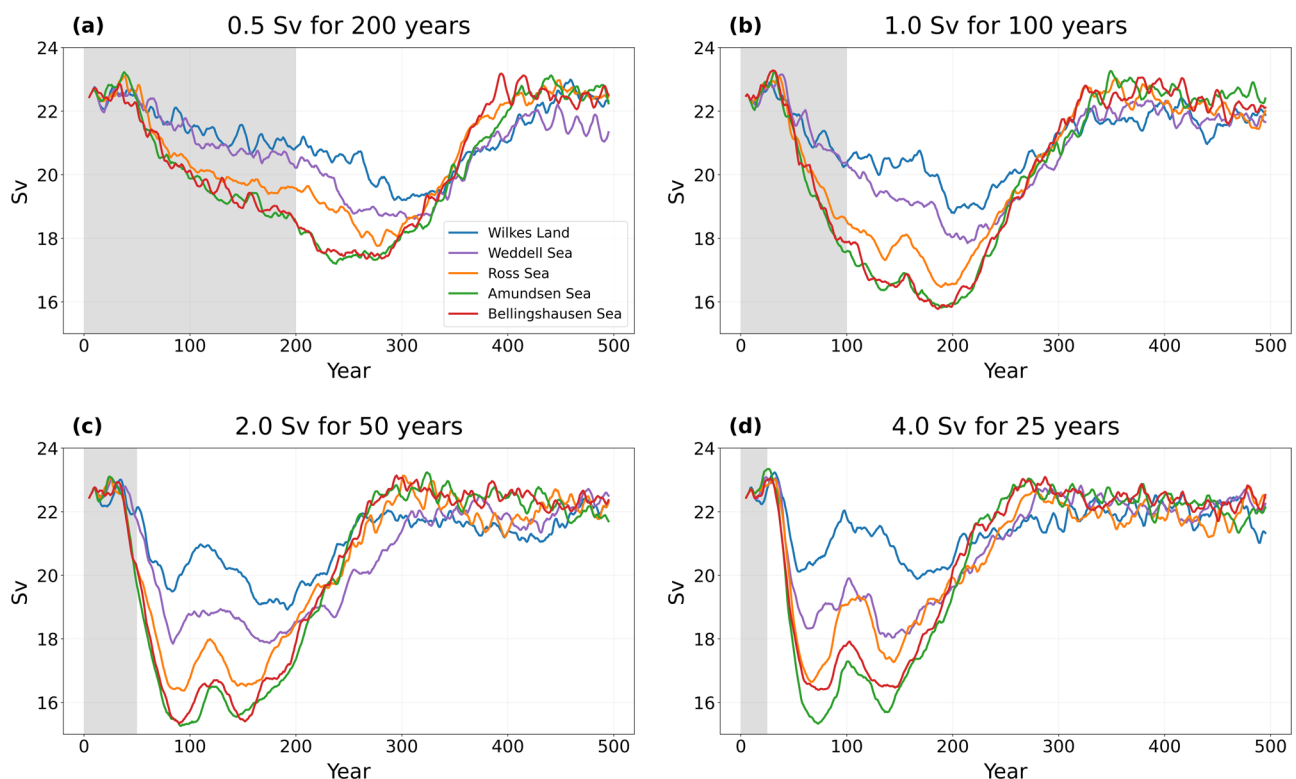


**Fig. 6 | AMOC response to different hosing durations.** **a** Response of AMOC to the freshwater hosing of 0.5 Sv for 200 years, applied over a designated area of Southern Ocean. AMOC index was computed based on mean meridional stream function (Sv) in Atlantic Ocean. The area of the imposed freshwater is indicated as the different

colored line as indicated in the lower right corner. **b–d** As in (a) except for the freshwater hosing of 1.0 Sv for 100 years, 2.0 Sv for 50 years, and 4.0 Sv for 25 years, respectively. The hosing periods are indicated by a light gray shading.

density gradient through a deep-water adjustment<sup>12</sup>. This finding appears to contradict the current study. However, the effect of WAIS melting on AMOC depends on whether GrIS melting is involved<sup>1</sup>. In our study, due to the absence of GrIS melting, the SO freshwater can readily transport to the Northern Hemisphere through a global ocean adjustment process<sup>12,22</sup>. Conversely, as GrIS melting is involved, the northward transport of SO freshwater may weaken due to a reduced meridional density gradient. However, the impact of GrIS melting on AMOC tipping is not solely determined by the presence or absence of melting but rather by its magnitude and duration. The effect of the slow melting of GrIS on AMOC could be overwhelmed by the abrupt and/or massive melting of WAIS. Therefore, further studies are needed to better understand how the competing or combined effects of GrIS and WAIS melting influence AMOC stability, especially in a future climate. These studies should consider systematic changes in the amplitude, duration, and timing of each ice sheet's melting. Finally, attaining a comprehensive understanding of the AMOC response to future climate change requires an in-depth analysis on the complex feedback processes involving ice-dynamics, atmospheric teleconnections, and ocean circulation.

Although LOVECLIM has been known to be capable to investigate intrinsic mechanisms of AMOC variation<sup>21,23–27</sup>, some factors that affect AMOC may be less reliable. This is because the ocean model has a low resolution and parameterizes ocean eddies, and the atmospheric model is a simple quasi-geostrophic model (“Methods” section). As such, the low-resolution ocean model may not be enough to simulate the eddy compensation effect in AABW, even though the isopycnal-mixing formulation and the eddy-induced advection were implemented in the ocean model<sup>28</sup> (“Methods” section). From the bipolar ocean seesaw perspective, which suggests that a decrease in deep-water formation in one hemisphere can lead to an increase in deep-water formation in the other, the formation of AABW is negatively correlated with the formation of NADW<sup>12,29,30</sup>. Therefore, the realism with which the parameterizations in LOVECLIM simulates the eddy effect on AABW formation may impact the AMOC's response to SO hosing. Accurate simulation of precipitation, particularly over the subtropical Atlantic Ocean, is necessary to correctly assess the impact of SO cooling on subtropical Atlantic surface salinity. The LOVECLIM simulation of the current climatological mean of zonal mean precipitation accurately captured both its location and magnitude. However, the simulated pattern exhibited a rather symmetric distribution between the hemispheres<sup>28</sup>. These shortcomings necessitate a cautious interpretation of the results presented in this study. Nevertheless, the competing processes in the deep ocean between AABW export and NADW export near 32° S are not the primary mechanisms proposed in this study; and the strong relationship between the enhanced hemispheric thermal contrast due to SO cooling and the northward shift of ITCZ is governed by dynamic principles, although LOVECLIM tends to simulate a somewhat symmetric precipitation distribution between the hemispheres. Therefore, our conclusions based on LOVECLIM remain reasonable and broadly applicable.

## Methods

### LOVECLIM configurations

LOVECLIM1.3<sup>28</sup> was utilized in this study. This model consists of the atmospheric model solving a quasi-geostrophic potential vorticity equation with horizontal T21 truncation, equivalent to a horizontal resolution of  $\sim 5.6^\circ \times 5.6^\circ$  and three vertical levels, at 800, 500, and 200 hPa (ECBilt<sup>31</sup>); the ocean model solving a primitive equation of ocean and sea ice model (CLIO<sup>32</sup>) with a horizontal resolution of  $3^\circ \times 3^\circ$  and 20 vertical levels, which are unevenly stratified over a depth of 5500 m; a vegetation model (VECODE<sup>33</sup>) having two types of plant function. In CLIO, the vertical mixing parameterization<sup>32</sup> with a simplified turbulence closure scheme<sup>34</sup> and an isopycnal-mixing process to capture the effect of mesoscale eddies on the transport<sup>35</sup> are included. The ice sheet and the carbon cycle models were deactivated. The control experiment was conducted under a pre-industrial condition, including the specific orbital

parameters (eccentricity = 0.016724, obliquity = 23.446°, argument of perihelion = 102.04°), the solar constant of  $1365 \text{ W m}^{-2}$ , and fixed greenhouse gas concentrations ( $\text{CO}_2 = 276.72 \text{ ppm}$ ,  $\text{CH}_4 = 663.5 \text{ ppb}$ , the  $\text{N}_2\text{O} = 265.8 \text{ ppb}$ ). In this study, the last 100 years of a 900-year run following spin-up were utilized. Regarding the performance, LOVECLIM has been widely used for investigating intrinsic mechanisms of AMOC variation<sup>21,23–27</sup>.

### Horizontal salinity flux convergence and surface flux of salinity

The salinity flux convergence and surface salinity flux are computed as  $-\left[\frac{\partial(uS)}{\partial x} + \frac{\partial(vS)}{\partial y}\right]$  and  $\frac{E-P}{h} [S]$ , respectively, following An et al.<sup>36</sup>. Here,  $u$  and  $v$  represents zonal and meridional velocities, respectively.  $S$  is salinity,  $E$  is evaporation,  $P$  is precipitation, and  $h$  is the mixed-layer depth. The yearly mean data are used for the computations. Notably, the square bracket denotes the depth average over the mixed layer.

### Reporting summary

Further information on research design is available in the Nature Portfolio Reporting Summary linked to this article.

### Data availability

LOVECLIM code is available at <https://www.elic.ucl.ac.be/modx/index.php?id=289>, and the model simulations utilized in this study are available at <https://data.mendeley.com/datasets/cj7vckdz/1>.

Received: 3 June 2024; Accepted: 30 August 2024;

Published online: 07 September 2024

## References

- Ivanovic, R. F., Gregoire, L. J., Wickert, A. D. & Burke, A. Climatic effect of Antarctic meltwater overwhelmed by concurrent northern hemispheric melt. *Geophys. Res. Lett.* **45**, 5681–5689 (2018).
- Weaver, A. J., Saenko, O. A., Clark, P. U. & Mitrovica, J. X. Meltwater pulse 1A from Antarctica as a trigger of the Bolling-Allerød warm interval. *Science* **299**, 1709–1713 (2003).
- Rintoul, S. R. Rapid freshening of Antarctic Bottom Water formed in the Indian and Pacific oceans. *Geophys. Res. Lett.* **34**, L06606 (2007).
- An, S.-I., Kim, H. & Kim, B.-M. Impact of freshwater discharge from the Greenland ice sheet on North Atlantic climate variability. *Theor. Appl. Climatol.* **112**, 29–43 (2013).
- Menezes, V. V., Macdonald, A. M. & Schatzman, C. Accelerated freshening of Antarctic Bottom Water over the last decade in the Southern Indian Ocean. *Sci. Adv.* **3**, e1601426 (2017).
- Silvano, A. et al. Freshening by glacial meltwater enhances melting of ice shelves and reduces formation of Antarctic Bottom Water. *Sci. Adv.* **4**, eaap9467 (2018).
- McKay, D. I. A. et al. Exceeding 1.5 °C global warming could trigger multiple climate tipping points. *Science* **377**, eabn7950 (2022).
- Richardson, G., Wadley, M. R., Heywood, K. J., Stevens, D. P. & Banks, H. T. Short-term climate response to a freshwater pulse in the Southern Ocean. *Geophys. Res. Lett.* **32**, L03702 (2005).
- Ma, H. & Wu, L. Global teleconnections in response to freshening over the Antarctic Ocean. *J. Clim.* **24**, 1071–1088 (2011).
- Menviel, L., Timmermann, A., Timm, O. E. & Mouchet, A. Climate and biogeochemical response to a rapid melting of the West Antarctic Ice Sheet during interglacials and implications for future climate. *Paleoceanography* **25**, PA4231 (2010).
- Stouffer, R. J., Seidov, D. & Haupt, B. J. Climate response to external sources of freshwater: North Atlantic versus the Southern Ocean. *J. Clim.* **20**, 436–448 (2007).
- Swingedouw, D., Fichefet, T., Goosse, H. & Loutre, M. F. Impact of transient freshwater releases in the Southern Ocean on the AMOC and climate. *Clim. Dyn.* **33**, 365–381 (2009).



13. Trevena, J., Sijp, W. P. & England, M. H. Stability of Antarctic Bottom Water formation to freshwater fluxes and implications for global climate. *J. Clim.* **21**, 3310–3326 (2008).
14. van de Wal, R. S. W. et al. A high-end estimate of sea level rise for practitioners. *Earth's Future* **10**, e2022EF002751 (2022).
15. Chylek, P., Folland, C. K., Lesins, G. & Dubey, M. K. Twentieth century bipolar seesaw of the Arctic and Antarctic surface air temperatures. *Geophys. Res. Lett.* **37**, L08703 (2010).
16. Sinet, S., von der Heydt, A. S. & Dijkstra, H. A. AMOC stabilization under the interaction with tipping polar ice sheets. *Geophys. Res. Lett.* **50**, e2022GL100305 (2023).
17. Lee, S.-K. et al. Human-induced changes in the global meridional overturning circulation are emerging from the Southern Ocean. *Commun. Earth. Environ.* **4**, 69 (2023).
18. Toggweiler, J. R. & Samuels, B. Effects of the westerly wind stress over the Southern Ocean on the meridional overturning. *Deep Sea Res.* **42**, 477–500 (1995).
19. Deschamps, P. et al. Ice-sheet collapse and sea-level rise at the Bølling warming 14,600 years ago. *Nature* **483**, 559–564 (2012).
20. Bentley, M. J. et al. A community-based geological reconstruction of Antarctic Ice Sheet deglaciation since the Last Glacial Maximum. *Quat. Sci. Rev.* **100**, 1–9 (2014).
21. Jackson, L. C. et al. Global and European climate impacts of a slowdown of the AMOC in a high resolution GCM. *Clim. Dyn.* **45**, 3299–3316 (2015).
22. Timmermann, A., An, S.-I., Krebs, U. & Goosse, H. ENSO suppression due to weakening of the North Atlantic thermohaline circulation. *J. Clim.* **18**, 3122–3139 (2005).
23. Driesschaert, E. et al. Modeling the influence of Greenland ice sheet melting on the Atlantic meridional overturning circulation during the next millennia. *Geophys. Res. Lett.* **34**, L10707 (2007).
24. Krebs, U. & Timmermann, A. Fast advective recovery of the Atlantic meridional overturning circulation after a Heinrich event. *Paleoceanography* **22**, PA1220 (2007).
25. Timmermann, A. et al. The influence of a weakening of the Atlantic meridional overturning circulation on ENSO. *J. Clim.* **20**, 4899–4919 (2007).
26. Friedrich, T. et al. The mechanism behind internally generated centennial-to-millennial scale climate variability in an earth system model of intermediate complexity. *Geosci. Model Dev.* **3**, 377–389 (2010).
27. An, S.-I., Kim, H.-J. & Kim, S.-K. Rate-dependent hysteresis of the Atlantic meridional overturning circulation system and its asymmetric loop. *Geophys. Res. Lett.* **48**, e2020GL090132 (2021).
28. Goosse, H. et al. Description of the Earth system model of intermediate complexity LOVECLIM version 1.2. *Geosci. Model Dev.* **3**, 603–633 (2010).
29. Seidov, D., Stouffer, R. J. & Haupt, B. J. Meltwater and the global ocean conveyor: northern versus southern connections. *Glob. Planet. Change* **30**, 257–270 (2001).
30. Brix, H. & Gerdes, R. Influence of high-latitude surface forcing on the global thermohaline circulation. *J. Geophys. Res.* **108**, 3022 (2003).
31. Opsteegh, J. D., Haarsma, R. J., Selten, F. M., Kattenberg, A. & ECBILT A dynamic alternative to mixed boundary conditions in ocean models. *Tellus A Dyn. Meteorol. Oceanogr.* **50**, 348–367 (1998).
32. Goosse, H. & Fichefet, T. Importance of ice-ocean interactions for the global ocean circulation: a model study. *J. Geophys. Res. Oceans* **104**, 23337–23355 (1999).
33. Brovkin, V., Ganopolski, A. & Svirezhev, Y. A continuous climate-vegetation classification for use in climate-biosphere studies. *Ecol. Model.* **101**, 251–261 (1997).
34. Mellor, G. & Yamada, T. Development of a turbulence closure model for geophysical fluid problems. *Rev. Geophys. Space Phys.* **20**, 851–875 (1982).
35. Gent, P. & McWilliams, J. Isopycnal mixing in ocean general circulation models. *J. Phys. Oceanogr.* **20**, 150–155 (1990).
36. An, S.-I. et al. Global cooling hiatus driven by an AMOC overshoot in a carbon dioxide removal scenario. *Earth's Future* **9**, e2021EF002165 (2021).

## Acknowledgements

This was supported by the National Research Foundation of Korea (NRF) grants funded by the Korean government (MSIT) (NRF-2018R1A5A1024958) and the Yonsei Signature Research Cluster Program of 2024-22-0162. S.I.A. was supported by the Yonsei Fellowship, funded by Lee Youn Jae. H.A.D. is funded by the European Research Council through the ERC-AdG Project TAOC (Project 101055096).

## Author contributions

S.I.A. coordinated and wrote a draft of the paper. J.Y.M. performed the model experiment and analyzed the results. S.I.A., J.Y.M., H.A.D., Y.M.Y., and H.S. discussed the results and reviewed the paper.

## Competing interests

The authors declare no competing interests.

## Additional information

**Supplementary information** The online version contains supplementary material available at <https://doi.org/10.1038/s43247-024-01670-7>.

**Correspondence** and requests for materials should be addressed to Soon-Il An.

**Peer review information** *Communications Earth & Environment* thanks Matthew Collins and the other, anonymous, reviewer(s) for their contribution to the peer review of this work. Primary Handling Editor: Alireza Bahadori. A peer review file is available.

**Reprints and permissions information** is available at <http://www.nature.com/reprints>

**Publisher's note** Springer Nature remains neutral with regard to jurisdictional claims in published maps and institutional affiliations.

**Open Access** This article is licensed under a Creative Commons Attribution-NonCommercial-NoDerivatives 4.0 International License, which permits any non-commercial use, sharing, distribution and reproduction in any medium or format, as long as you give appropriate credit to the original author(s) and the source, provide a link to the Creative Commons licence, and indicate if you modified the licensed material. You do not have permission under this licence to share adapted material derived from this article or parts of it. The images or other third party material in this article are included in the article's Creative Commons licence, unless indicated otherwise in a credit line to the material. If material is not included in the article's Creative Commons licence and your intended use is not permitted by statutory regulation or exceeds the permitted use, you will need to obtain permission directly from the copyright holder. To view a copy of this licence, visit <http://creativecommons.org/licenses/by-nc-nd/4.0/>.

© The Author(s) 2024